sensors

MDPI

Article

Consensus Tracking of Nonlinear Agents Using Distributed Nonlinear Dynamic Inversion with Switching Leader-Follower Connection

Sabyasachi Mondal * and Antonios Tsourdos

School of Aerospace, Transport and Manufacturing (SATM), Cranfield University, Cranfield MK43 0AL, UK
* Correspondence: sabyasachi.mondal@cranfield.ac.uk

Abstract: In this paper, a consensus tracking protocol for nonlinear agents is presented, which is based on the Nonlinear Dynamic Inversion (NDI) technique. Implementation of such a technique is new in the context of the consensus tracking problem. The tracking capability of nonlinear dynamic inversion (NDI) is exploited for a leader-follower multi-agent scenario. We have provided all the mathematical details to establish its theoretical foundation. Additionally, a convergence study is provided to show the efficiency of the proposed controller. The performance of the proposed controller is evaluated in the presence of both (a) random switching topology among the agents and (b) random switching of leader–follower connections, which is realistic and not reported in the literature. The follower agents track various trajectories generated by a dynamic leader, which describes the tracking capability of the proposed controller. The results obtained from the simulation study show how efficiently this controller can handle the switching topology and switching leader-follower connections.

Keywords: consensus tracking; distributed nonlinear dynamic inversion; leader–follower consensus

Citation: Mondal , S.; Tsourdos, A. Consensus Tracking of Nonlinear Agents Using Distributed Nonlinear Dynamic Inversion with Switching Leader-Follower Connection. *Sensors* **2022**, *22*, 9537. https://doi.org/10.3390/s22239537

Academic Editor: Yuan Yao

Received: 18 October 2022
Accepted: 30 November 2022
Published: 6 December 2022

1. Introduction

Multiple UAV or multi-agent operation has been an exciting research area for years. Multi-agent systems (MASs) play an important role in executing complex tasks, which are usually difficult for a single UAV or agent. Examples of MASs applications are cooperative mobile robotics [1], sensory networks [2], flocking [3], formation control of robot teams [4], rendezvous of multiple spacecraft [5], etc. Agents share information over a communication network and take appropriate control action to agree on a decision, i.e., they achieve consensus. The control action is generated by consensus protocols designed using control theory. Researchers have proposed a variety of consensus protocols to solve different categories of consensus problems considering linear and nonlinear agents, like communication issues (switching topology [6–8], delays [9–11], noise [12–14]), disturbance [15,16], and fault [17,18].

A significant number of these protocols achieve the consensus with a single value, which primarily depends on the initial values of the agents. However, in a real-world scenario, the agents may need to converge to a time-varying consensus value, which is available to a few agents of networked MASs. This problem can be categorized as a consensus tracking problem (also known as a leader–follower consensus problem because a leader agent provides the time-varying values). Leader–follower consensus protocols have been proposed to solve this problem. In [19], the authors considered the nearest neighborhood principle and showed that all agents' states converged to the leader's state if the agents were jointly connected to the leader. However, this scheme was too restrictive. Ren and Beard [20] addressed the same problem in [19] with directed topology and relaxed restriction on the topology. Ren [21] showed that the consensus protocol of a proportional and derivative type could track a time-varying reference state of a virtual leader, but a proportional-like consensus protocol cannot do it. Peng et al. [22] solved a leader–following consensus

problem. The leader agent has varying velocity and time-varying delays. Cao et al. [23] presented leader–follower consensus using a variable structure method. Hong et al. [24] proposed a distributed output regulation algorithm for linear agents. In [25], the authors solved a consensus problem for unknown systems. Wang et al. [26] used a distributed observer to solve an adaptive leader–follower consensus problem for higher-order agents. In [27], the authors addressed fixed-time event/self-triggered leader–follower consensus problems for networked multi-agent systems having nonlinear dynamics. In [28], the authors proposed distributed adaptive protocol for cooperative tracking problem considering pure relative output information. Guo et al. [29] discussed a fixed-time consensus tracking problem of nonlinear agents via discontinuous protocols. In [30], the adaptive consensus tracking control problem of nonlinear multi-agent systems (MASs) is solved using a robust adaptive event-triggered sliding-mode control method. Additionally, the authors considered unknown perturbations and limited network bandwidth in the problem.

One of the significant events that cause the tracking failure is the actuator fault. There exist a few papers that addressed the actuator fault in the consensus tracking problem. Qin et al. [31] implemented sliding mode control to solve the consensus tracking problem of nonlinear agents with actuator faults. They also considered disturbance in their study. Mu et al. [32] proposed an event-triggered control strategy to solve the leader–following consensus problem of agents with time-varying actuator faults. Xia et al. [33] presented a fault-tolerant fuzzy tracking controller for nonlinear agents subject to actuator failures and external disturbances. Gong et al. [34] studied an adaptive cooperative fault-tolerant supervisory control problem for nonlinear leader–follower agents with unknown control coefficients and actuator faults. More results can be found in [35,36]. Along with the actuator fault, switching topology is another event that is practical and causes difficulties during the consensus process. A few works have been reported in the literature where the effect of switching topology in tracking is studied. Wen et al. [6] presented consensus Tracking of agents having Lipschitz node dynamics and switching Topologies. Wang et al. [37] addressed a H_∞ consensus tracking control problem for linear agents. They considered switching topology and disturbances in their study. Razaq et al. [38] presented a leader-based consensus of one-sided Lipschitz (OSL) agents under switching graphs and input saturation. It can be mentioned that there exist a small number of papers that discussed consensus tracking considering both the switching topology and actuator fault. Sader et al. [39] presented the consensus tracking problem of agents' nonlinear function, exogenous disturbances, and actuator faults. They considered the switching communication topologies in their study. Liu et al. [40] designed a distributed fault-tolerant consensus tracking control for multi-agent systems with actuator faults considering both fixed and switching topologies. Additionally, Cao et al. [41] solved the same problem of consensus tracking control of stochastic agents with actuator fault under randomly switched topology.

It can be mentioned that, in the leader–follower or consensus tracking problem, the followers are connected to a few agents of the network. The connection between these followers and the leader can also change in a similar way in which the switching topology occurs. However, this leader–follower switching connection is not addressed in any paper. We will address this problem along with the actuator fault in this paper.

All of these papers implemented linear and nonlinear control theory to design the controller. There exists a control technique that is very efficient in designing controllers for nonlinear plants. The philosophy behind NDI is to use feedback linearization theory to remove the nonlinearities in the plant. Additionally, the response of the closed-loop plant is similar to a stable linear system. There are many advantages to using an NDI controller, e.g., (a) closed-form control expression, (b) easy mechanization, (c) global exponential stability, (d) inclusion of nonlinear kinematics in plant inversion, and (e) minimization of the need for individual gain tuning or gain scheduling. It has been used to design controllers in various applications. In [42], the authors designed an NDI-based flight controller. In [43], NDI controller was implemented for autonomous landing of UAV. Lifeng et al. [44] used Improved Dynamic Inversion to design trajectory tracking control for a quadrotor. In [45],

the authors used an NDI controller to present a flying formation scheme. The follower UAVs are used to track the desired attitude commanded by the leader. The attitude control of a flexible aircraft was described using dynamic inversion by Caverly et al. [46]. Another example of using NDI to solve an attitude control problem of a hovering quad tiltrotor eVTOL Vehicle was presented by Lombaerts et al. [47]. In [48], the authors used NDI to track the angular reference rates obtained from the guidance command in a missile guidance problem. In [49], the authors presented a Nonlinear Dynamic Inversion (NDI) based flight controller for a VTOL aircraft, including transition maneuvers. They used virtual controls, generalized forces and moments to control its longitudinal motion. A fault-tolerant control (FTC) scheme was proposed by Ma et al. [50]. The scheme was based on extended state observer (ESO) and nonlinear dynamic inversion (NDI). In [51], trajectory generation and control architecture for a fully autonomous autorotative flare are proposed. These flare trajectories are tracked by a nonlinear dynamic inversion (NDI) control law.

These papers present the implementation of dynamic inversion to design a controller for a single platform. Mondal et al. [14] proposed a distributed consensus protocol based on NDI and named it Distributed NDI or DNDI. It has been implemented to solve consensus problems with actuator fault [18], external disturbances [16], and bipartite consensus [52]. In this paper, we have proposed a variety of DNDI that exploits the tracking capability of NDI and successfully solves a leader–following consensus tracking problem, which is different from leaderless consensus in terms of concept and formulation. We have evaluated the performance of the proposed controller in the presence of both (a) switching topology among the agents and (b) switching connections between the leader and the followers.

The contribution in this paper is given as follows.

- Distributed Nonlinear Dynamic Inversion (DNDI) based control protocol is designed to address the consensus tracking problem of nonlinear agents for the first time. This is novel because we exploited the tracking capability of nonlinear dynamic inversion (NDI) for a leader-follower multi-agent scenario.
- Detailed mathematical derivation of the controller is provided.
- Mathematical details for convergence study are presented, which gives proof of its correctness.
- We have considered the presence of both (a) switching topology among the agents and (b) switching connection between the leader and the followers to make the scenario more realistic. This is new in the context of the consensus tracking problem.
- Realistic simulation study shows the accuracy of the proposed controller. Different types of leader trajectories are generated to demonstrate the tracking capability of the proposed controller.

The rest of the paper is organized as follows. In Section 2, the preliminaries are given. In Section 3, the problem description is presented. Mathematical details of tracking DNDI for leader–follower consensus tracking is shown in Section 4. The convergence study of tracking DNDI is presented in Section 5. Simulation results are shown in Section 6, and Section 7 gives the conclusion.

2. Preliminaries

In this section, we have presented a few topics that are relevant to this study.

2.1. Consensus Tracking of Multiple Agents

Let us consider N nonlinear agents connected by a communication topology. The agents (called followers) need to track the trajectory of a leader $X_L(t)$, which is connected to a few agents of the networked agents. If the followers' states, i.e., $X_i(t)$; $i = 1, 2, \ldots, N$ achieve the consensus and track the leader's states, i.e., if for any initial conditions $\lim_{t\to\infty} |X_i(t) \to X_L(t)| = 0$, the followers are considered to achieve consensus tracking.

2.2. Graph Theory

The communication among the agents can be represented by a weighted graph written by $\mathcal{G} = \{\mathcal{V}, \mathcal{E}\}$. The vertices $\mathcal{V} = \{v_1, v_2, \ldots, v_N\}$ of the graph are used to represent the agents. The set of edges, i.e., $\mathcal{E} \subseteq \mathcal{V} \times \mathcal{V}$, shows the communication among the agents. The elements of weighted adjacency matrix $\mathcal{A} = [a_{ij}] \in \Re^{N\times N}$ of $\mathcal{G}$ are given by $a_{ij} > 0$ if $(v_j, v_i) \in \mathcal{E}$, otherwise $a_{ij} = 0$. There is no self-loop in the graph, i.e., the diagonal elements of the adjacency matrix $\mathcal{A}$ as zero ($a_{ii} = 0$). The degree matrix is represented as $\mathcal{D} \in \Re^{N\times N} = diag\{d_1\ d_2\ \ldots d_N\}$, where $d_i = \sum_{j\in N_i} a_{ij}$. The Laplacian matrix is written as $\mathcal{L} = \mathcal{D} - \mathcal{A}$. In this paper, we consider the topology $\mathcal{G}$ of the network as undirected (i.e., $a_{ij} = a_{ji}$) and connected ($v_i, v_j \in \mathcal{V}$, there exists a path from v_i to v_j).

2.3. Switching Leader-Follower Connection

In this paper, we have evaluated the performance of the proposed controller in the presence of a switching leader–follower connection along with the switching topology among the followers. In case of a consensus tracking problem, the leader's state information is available to a few follower agents. Let us consider the leader's state information is available to p agents, $p \subset N$, where N is the total number of followers. At any time $t \geq t_0$, the recipient followers are changed (some of them or all), and the leader's information is available to q agents ($p = q$ or $p \neq q$).

2.4. Lemma

The useful lemmas used in this paper are given as follows.

Lemma 1 ([20]). *The Laplacian matrix L in an undirected graph is semi-positive definite, it has a simple zero eigenvalue, and all the other eigenvalues are positive if and only if the graph is connected. Therefore, L is symmetric and it has N non-negative, real-valued eigenvalues* $0 = \lambda_1 \leq \lambda_2 \leq \ldots \leq \lambda_N$.

Lemma 2 ([53]). *Let* $\psi_1(t), \psi_2(t) \in R^m$ *be continuous positive vector functions, by Cauchy inequality and Young's inequality, there exists the following inequality:*

$$\begin{aligned} \psi_1(t)\psi_2(t) &\leq \| \psi_1(t) \| \| \psi_2(t) \| \\ &\leq \frac{\| \psi_1(t) \|^{\bar{\lambda}}}{\bar{\lambda}} + \frac{\| \psi_2(t) \|^{\bar{\zeta}}}{\bar{\zeta}} \end{aligned} \tag{1}$$

where

$$\frac{1}{\bar{\lambda}} + \frac{1}{\bar{\zeta}} = 1$$

Lemma 3 ([54]). *Let* $R(t) \in \Re$ *be a continuous positive function with bounded initial* $R(0)$. *If the inequality holds* $\dot{R}(t) \leq -\nu R(t) + \varsigma$ *where,* $\nu > 0, \varsigma > 0$, *then the following inequality holds.*

$$R(t) \leq R(0)e^{-\nu t} + \frac{\varsigma}{\nu}\left(1 - e^{-\nu t}\right) \tag{2}$$

3. Problem Formulation

In this section, the problem definition is given. The objective is to design a consensus tracking protocol that enables a class of nonlinear agents' (follower) states $X_i(t)$; $i = 1, 2, \ldots, N$ to achieve the consensus and track the desired signal ($X_L(t)$) generated by a leader agent, i.e., $X_i(t) \to X_L(t)$. The ith follower agent is described by

$$\dot{X}_i = f(X_i) + g(X_i)U_i \tag{3}$$

$$Y_i = X_i \tag{4}$$

where, $X_i \in \Re^n$, $U_i \in \Re^n$ are states and control, respectively. f is a continuously differentiable vector-valued function representing the nonlinear dynamics.

Assumption 1. *The matrix $g(X_i)$ is invertible for all time.*
The leader dynamics is given by

$$\dot{X}_L(t) = f_L(X_L(t), t) \tag{5}$$

where, $X_L \in \Re^n$. f_L is piecewise continuous in t.

Assumption 2. *$X_L(t)$ and $\dot{X}_L(t)$ are assumed to be bounded.*

It can be mentioned that the leader's state information is available to a few agents of the networked agents.

4. Distributed Nonlinear Dynamic Inversion for Consensus Tracking

Considering the agent (Equations (3) and (4)) and leader dynamics (Equation (5)), the consensus tracking error of i^{th} agent (scalar $n = 1$) is given by

$$e_i = \sum_{j \in N_i} a_{ij}(x_i - x_j) + \beta_i(x_i - x_L) \tag{6}$$

Simplifying Equation (6), we obtain

$$e_i = (d_i + \beta_i)x_i - a_i X - \beta_i x_L \tag{7}$$

where $X \in \Re^N$, x_L defines the state of a scalar agent, and β_i shows if ith agent is connected to the leader. The tracking error is given for the agents with state vector $X_i \in \Re^n; n > 1$.

$$E_i = (\bar{d}_i + \bar{\beta}_i)X_i - \bar{a}_i \mathbf{X} - \bar{\beta}_i X_L \tag{8}$$

where $E_i \in \Re^n$, $\bar{d}_i = (d_i \otimes \mathbf{I}_n) \in \Re^{n \times n}$, $\bar{a}_i = (a_i \otimes \mathbf{I}_n) \in \Re^{n \times nN}$, $\bar{\beta}_i = (\beta_i \otimes \mathbf{I}_n) \in \Re^{n \times n}$, $X_L \in \Re^n$, and $\mathbf{X} = [X_1^T \; X_2^T \; \dots \; X_N^T]^T \in \Re^{nN}$. We enforce the first-order error dynamics as follows.

$$\dot{E}_i + K_i E_i = 0 \tag{9}$$

Differentiation of Equation (9) gives

$$\begin{aligned} \dot{E}_i &= (\bar{d}_i + \bar{\beta}_i)\dot{X}_i - \bar{a}_i \dot{\mathbf{X}} - \bar{\beta}_i \dot{X}_L \\ &= (\bar{d}_i + \bar{\beta}_i)[f(X_i) + g(X_i)U_i] - \bar{a}_i \dot{\mathbf{X}} - \bar{\beta}_i \dot{X}_L \end{aligned} \tag{10}$$

The expressions of E_i and $\dot{E}_i$ are substituted in Equation (9) to obtain

$$(\bar{d}_i + \bar{\beta}_i)[f(X_i) + g(X_i)U_i] - \bar{a}\dot{\mathbf{X}} - \bar{\beta}_i \dot{X}_L + K_i\big((\bar{d}_i + \bar{\beta}_i)X_i - \bar{a}_i \mathbf{X} - \bar{\beta}_i X_L\big) = 0 \tag{11}$$

Control U_i of ith agent is obtained by simplifying Equation (11) as follows.

$$U_i = (g(X_i))^{-1}\left[- f(X_i) + (\bar{d}_i + \bar{\beta}_i)^{-1}\left(\bar{a}_i \dot{\mathbf{X}} + \bar{\beta}_i \dot{X}_L - K_i\left((\bar{d}_i + \bar{\beta}_i)X_i - \bar{a}_i \mathbf{X} - \bar{\beta}_i X_L\right)\right)\right] \tag{12}$$

5. Convergence Study of DNDI for Consensus Tracking

The convergence study of DNDI is presented here. We define a smooth scalar function:

$$\tilde{V} = \frac{1}{2}\mathbf{X}^T(\tilde{L} \otimes \mathbf{I}_n)\mathbf{X} \tag{13}$$

$\tilde{L} \otimes \mathbf{I}_n$ can be represented by

$$\tilde{L} \otimes \mathbf{I}_n = \tilde{S}\Omega\tilde{S}^T \tag{14}$$

where, $\tilde{S} \in \Re^{nN \times nN}$ is the left eigenvalue matrix of $\tilde{L} \otimes \mathbf{I}_n$, $\Omega = \big(diag\{0, \lambda_2(\tilde{L}), \lambda_3(\tilde{L}), \ldots, \lambda_N(\tilde{L})\} \otimes \mathbf{I}_n\big) \in \Re^{nN \times nN}$ is eigenvalue matrix, $\tilde{S}^T\tilde{S} = \tilde{S}\tilde{S}^T = \mathbf{I}_{nN \times nN}$.

$$\begin{aligned}
\tilde{V} &= \frac{1}{2}\mathbf{X}^T(\tilde{L} \otimes \mathbf{I}_n)\mathbf{X} \\
&= \frac{1}{2}\mathbf{X}^T\tilde{S}\Omega\tilde{S}^T\mathbf{X} \\
&= \frac{1}{2}\mathbf{X}^T\tilde{S}\sqrt{\Omega}\sqrt{\Omega}\tilde{S}^T\mathbf{X} \\
&= \frac{1}{2}\mathbf{X}^T\tilde{S}\sqrt{\Omega\bar{\Omega}}\sqrt{\bar{\Omega}^{-1}}\sqrt{\bar{\Omega}^{-1}}\sqrt{\bar{\Omega}\Omega}\tilde{S}^T\mathbf{X} \\
&= \frac{1}{2}\mathbf{X}^T\tilde{S}\Omega\bar{\Omega}^{-1}\Omega\tilde{S}^T\mathbf{X} \\
&= \frac{1}{2}\mathbf{X}^T\tilde{S}\Omega\Big(\tilde{S}^T\tilde{S}\Big)\bar{\Omega}^{-1}\Big(\tilde{S}^T\tilde{S}\Big)\Omega\tilde{S}^T\mathbf{X} \\
&= \frac{1}{2}\mathbf{X}^T\Big(\tilde{S}\Omega\tilde{S}^T\Big)\Big(\tilde{S}\bar{\Omega}^{-1}\tilde{S}^T\Big)\Big(\tilde{S}\Omega\tilde{S}^T\Big)\mathbf{X} \\
&= \frac{1}{2}\mathbf{X}^T(\tilde{L} \otimes \mathbf{I}_n)\Phi(\tilde{L} \otimes \mathbf{I}_n)\mathbf{X} \\
&= \frac{1}{2}\mathbf{E}^T\Phi\mathbf{E}
\end{aligned} \tag{15}$$

where $\bar{\Omega} = (diag\{\lambda_2(L), \lambda_2(L), \lambda_3(L), \ldots, \lambda_N(L)\} \otimes \mathbf{I}_n) \in \Re^{nN \times nN}$, $\mathbf{E} = [E_1^T\ E_2^T\ \ldots\ E_N^T]^T \in \Re^{nN}$, and $\Phi = \tilde{S}\bar{\Omega}^{-1}\tilde{S}^T \in \Re^{nN \times nN}$.

Remark 1. *Using Equations* (13) *and* (15)*, we can write*

$$\frac{\lambda_{min}(\Phi)}{2} \parallel \boldsymbol{E} \parallel^2 \leq V \leq \frac{\lambda_{max}(\Phi)}{2} \parallel \boldsymbol{E} \parallel^2 \tag{16}$$

$$\tilde{V} = \frac{1}{2}\mathbf{X}^T(\tilde{L} \otimes \mathbf{I}_n)\mathbf{X} = \frac{1}{2}\mathbf{X}^T\boldsymbol{E} \tag{17}$$

Remark 2. *According to Lemma 1,* $\lambda_2 > 0$*. Hence,* $\bar{\Omega}$ *is invertible.*

Remark 3. $\Phi = \tilde{S}\bar{\Phi}^{-1}\tilde{S}^T$ *is positive definite matrix. Hence,* $\tilde{V}$ *is positive definite subject to consensus error and qualify for a Lyapunov function.*

Differentiating Equation (13), we get

$$\dot{\tilde{V}} = \mathbf{X}^T(\tilde{L} \otimes \mathbf{I}_n)\dot{\mathbf{X}} = \mathbf{E}^T\dot{\mathbf{X}} = \sum_{i=1}^{N} E_i^T\Big[f(X_i) + g(X_i)U_i\Big] \tag{18}$$

where, $\mathbf{E} = [E_1^T\ E_2^T\ \ldots\ E_N^T]^T \in \Re^{nN}$. Substituting the control U_i expression in Equation (18) yields

$$\begin{aligned}
\dot{\tilde{V}} &= \sum_{i=1}^{N} E_i^T\Big[\big(\bar{d}_i + \bar{\beta}_i\big)^{-1}\big(\bar{a}_i\dot{\mathbf{X}} + \bar{\beta}_i\dot{X}_L - K_iE_i\big)\Big] \\
&= -\sum_{i=1}^{N} E_i^T\big(\bar{d}_i + \bar{\beta}_i\big)^{-1}K_iE_i + \sum_{i=1}^{N} E_i^T\big(\bar{d}_i + \bar{\beta}_i\big)^{-1}\bar{a}_i\dot{\mathbf{X}} \\
&+ \sum_{i=1}^{N} E_i^T\big(\bar{d}_i + \bar{\beta}_i\big)^{-1}\bar{\beta}_i\dot{X}_L
\end{aligned} \tag{19}$$

According to Lemma 2, we can write $E_i^T\left(\bar{d}_i+\bar{\beta}_i\right)^{-1}\bar{a}_i\dot{\mathbf{X}} \leq \| E_i \| \| \left(\bar{d}_i+\bar{\beta}_i\right)^{-1}\bar{a}_i\dot{\mathbf{X}} \|$

$$\leq \frac{\| E_i \|^2}{2} + \frac{\| \left(\bar{d}_i+\bar{\beta}_i\right)^{-1}\bar{a}_i\dot{\mathbf{X}} \|^2}{2} \tag{20}$$

and

$$E_i^T\left(\bar{d}_i+\bar{\beta}_i\right)^{-1}\bar{\beta}_i\dot{X}_L \leq \| E_i \| \| \left(\bar{d}_i+\bar{\beta}_i\right)^{-1}\bar{\beta}_i\dot{X}_L \| \leq \frac{\| E_i \|^2}{2} + \frac{\| \left(\bar{d}_i+\bar{\beta}_i\right)^{-1}\bar{\beta}_i\dot{X}_L \|^2}{2} \tag{21}$$

Substituting the inequality relation in Equation (19)

$$\dot{\tilde{V}} \leq \sum_{i=1}^{N}\left[- E_i^T\left(\bar{d}_i+\bar{\beta}_i\right)^{-1}K_iE_i + \| E_i \|^2 + \frac{\| \left(\bar{d}_i+\bar{\beta}_i\right)^{-1}\bar{a}_i\dot{\mathbf{X}} \|^2}{2} + \frac{\| \left(\bar{d}_i+\bar{\beta}_i\right)^{-1}\bar{\beta}_i\dot{X}_L \|^2}{2}\right] \tag{22}$$

Let us design the gain K_i as follows.

$$K_i = \left(\bar{d}_i+\bar{\beta}_i\right)\left(1+\frac{\alpha_i}{2}\lambda_{max}(\Phi)\right) \tag{23}$$

Equation (22) is written as

$$\begin{aligned}\dot{\tilde{V}} &\leq \sum_{i=1}^{N}\left[- \frac{\alpha_i}{2}\lambda_{max}(\Phi) \| E_i \|^2 + \frac{\| \left(\bar{d}_i+\bar{\beta}_i\right)^{-1}\bar{a}_i\dot{\mathbf{X}} \|^2}{2}\right. \\ &+ \left.\frac{\| \left(\bar{d}_i+\bar{\beta}_i\right)^{-1}\bar{\beta}_i\dot{X}_L \|^2}{2}\right] \\ &\leq -\alpha_i\tilde{V} + \tilde{\eta}\end{aligned} \tag{24}$$

where, $\tilde{\eta} = \frac{\|\left(\bar{d}_i+\bar{\beta}_i\right)^{-1}\bar{a}_i\dot{\mathbf{X}}\|^2}{2} + \frac{\|\left(\bar{d}_i+\bar{\beta}_i\right)^{-1}\bar{\beta}_i\dot{X}_L\|^2}{2}$. Applying Lemma 3 we obtain

$$\tilde{V} \leq \frac{\tilde{\eta}}{\alpha_i} + \left(\tilde{V}(0) - \frac{\tilde{\eta}}{\alpha_i}\right)e^{-\alpha_i t} \tag{25}$$

Therefore, it is clear that $\tilde{V}$ is bounded as $t \to \infty$. Moreover, we present the Uniformly Ultimate Boundedness (UUB) as follows.

Using Equations (16) and (25), and Lemma 1.2 presented by Ge et al. [54], we can write

$$\frac{\lambda_{min}(\Phi)}{2} \| \mathbf{E} \|^2 \leq \tilde{V} \leq \frac{\tilde{\eta}}{\alpha_i} + \left(\tilde{V}(0) - \frac{\tilde{\eta}}{\alpha_i}\right)e^{-\alpha_i t} \tag{26}$$

We can write Equation (26) as follows.

$$\begin{aligned}\frac{\lambda_{min}(\Phi)}{2} \| \mathbf{E} \|^2 &\leq \frac{\tilde{\eta}}{\alpha_i} + \left(\tilde{V}(0) - \frac{\tilde{\eta}}{\alpha_i}\right)e^{-\alpha_i t} \\ \| \mathbf{E} \| &\leq \sqrt{\frac{2\frac{\tilde{\eta}}{\alpha_i} + 2\left(\tilde{V}(0) - \frac{\tilde{\eta}}{\alpha_i}\right)e^{-\alpha_i t}}{\lambda_{min}(\Phi)}}\end{aligned} \tag{27}$$

It can be observed that, if $\tilde{V}(0) = \frac{\tilde{\eta}}{\alpha_i}$, then

$$\| \mathbf{E} \| \leq \kappa^* \tag{28}$$

$\forall t \geq 0$ and $\kappa^* = \sqrt{\frac{2\tilde{\eta}}{\alpha_i \lambda_{min}(\Phi)}}$. If $\tilde{V}(0) \neq \frac{\tilde{\eta}}{\alpha_i}$ then for any given $\kappa > \kappa^*$ there exist a time $\tilde{\tau} > 0$ such that $\forall t > \tilde{\tau}$, $\| \mathbf{E} \| \leq \kappa$.

$$\kappa = \sqrt{\frac{2\frac{\tilde{\eta}}{\alpha_i} + 2\left(\tilde{V}(0) - \frac{\tilde{\eta}}{\alpha_i}\right)e^{-\alpha_i T}}{\lambda_{min}(\Phi)}} \tag{29}$$

Therefore, we can write

$$\lim_{t \to \infty} \| \mathbf{E} \| = \kappa^* \tag{30}$$

Hence, it is proved that the error is bounded and the consensus tracking is successful.

6. Simulation Study

We have presented the simulation results and discussion in this section.

6.1. Agent Dynamics

We have considered ten agents ($N = 10$) for simulation. Highly nonlinear terms like sin and cos are included in the agents dynamics. The dynamics for ith agent [14] is given in Equations (31) and (32).

$$\dot{X}_{i_1} = X_{i_2} \sin(2X_{i_1}) + U_{i_1} \tag{31}$$

$$\dot{X}_{i_2} = X_{i_1} \cos(3X_{i_2}) + U_{i_2} \tag{32}$$

where, $X_i = \begin{bmatrix} X_{i_1} & X_{i_2} \end{bmatrix}^T$. The dynamics of Equations (31) and (32) are written in the form given in Equations (3) and (4) as follows.

$$f(X_i) = \begin{bmatrix} X_{i_2} \sin(2X_{i_1}) \\ X_{i_1} \cos(3X_{i_2}) \end{bmatrix} \tag{33}$$

and

$$g(X_i) = \begin{bmatrix} 1 & 0 \\ 0 & 1 \end{bmatrix} \tag{34}$$

and

$$U_i = \begin{bmatrix} U_{i_1} \\ U_{i_2} \end{bmatrix} \tag{35}$$

where $X_i \in \Re^2$. The states X_{1_i} of all the agents are denoted by $\mathbf{X}_1 = [X_{1_1}\ X_{2_1}\ \ldots\ X_{10_1}]$. Similarly, we denote $\mathbf{X}_2 = [X_{1_2}\ X_{2_2}\ \ldots\ X_{10_2}]$, $\mathbf{U}_1 = [U_{1_1}\ U_{2_1}\ \ldots\ U_{10_1}]$, and $\mathbf{U}_2 = [U_{1_2}\ U_{2_2}\ \ldots\ U_{10_2}]$. The errors in $\mathbf{X}_1$ and $\mathbf{X}_2$ is given by $\mathbf{E}$ *in* $\mathbf{X}_1$ and $\mathbf{E}$ *in* $\mathbf{X}_2$, respectively.

6.2. Communication Topology

The communication topology used in this simulation study is given as follows.

$$A = \begin{bmatrix} 0 & 0 & 1 & 1 & 1 & 1 & 0 & 1 & 1 & 1 \\ 0 & 0 & 0 & 0 & 0 & 0 & 0 & 1 & 0 & 1 \\ 1 & 0 & 0 & 0 & 0 & 0 & 1 & 0 & 0 & 1 \\ 1 & 0 & 0 & 0 & 1 & 1 & 0 & 0 & 0 & 1 \\ 1 & 0 & 0 & 1 & 0 & 1 & 0 & 1 & 0 & 0 \\ 1 & 0 & 0 & 1 & 1 & 0 & 1 & 1 & 1 & 0 \\ 0 & 0 & 1 & 0 & 0 & 1 & 0 & 1 & 1 & 0 \\ 1 & 1 & 0 & 0 & 1 & 1 & 1 & 0 & 0 & 1 \\ 1 & 0 & 0 & 0 & 0 & 1 & 1 & 0 & 0 & 1 \\ 1 & 1 & 1 & 1 & 0 & 0 & 0 & 1 & 1 & 0 \end{bmatrix} \tag{36}$$

The leader–follower connection is given by

$$\beta = \begin{bmatrix} 0 & 1 & 0 & 0 & 0 & 0 & 0 & 1 & 0 & 1 \end{bmatrix} \tag{37}$$

$\beta(i)$; $i = 1, 2, \ldots, N$ denotes the connection between leader with ith follower agent. β shows that the leader is connected to follower agents 2, 8, and 10.

6.3. Results and Discussion: Fixed Topology

We have considered two cases to describe the controller's performance. They are discussed in the following section.

6.3.1. Case 1: Leader States-Constant and Ramp Function

In this case, the leader dynamics are given as follows.

$$\dot{X}_{L_1} = 1 \tag{38}$$

$$\dot{X}_{L_2} = 0 \tag{39}$$

The consensus tracking controls $\mathbf{U}_1$ and $\mathbf{U}_2$, generated by the DNDI, are shown in Figures 1 and 2, respectively. These controls produce the state trajectories. The states of the leader (X_{L_1} and X_{L_2}) are ramp and constant functions, respectively. It can be seen that the agents' states $\mathbf{X}_1$ and $\mathbf{X}_2$ track the leader states X_{L_1} and X_{L_2}, respectively (shown in Figures 3 and 4). The states achieve consensus with values dictated by the leader. The consensus error $\mathbf{E}_i$ in states Figures 5 and 6 shows the tracking accuracy.

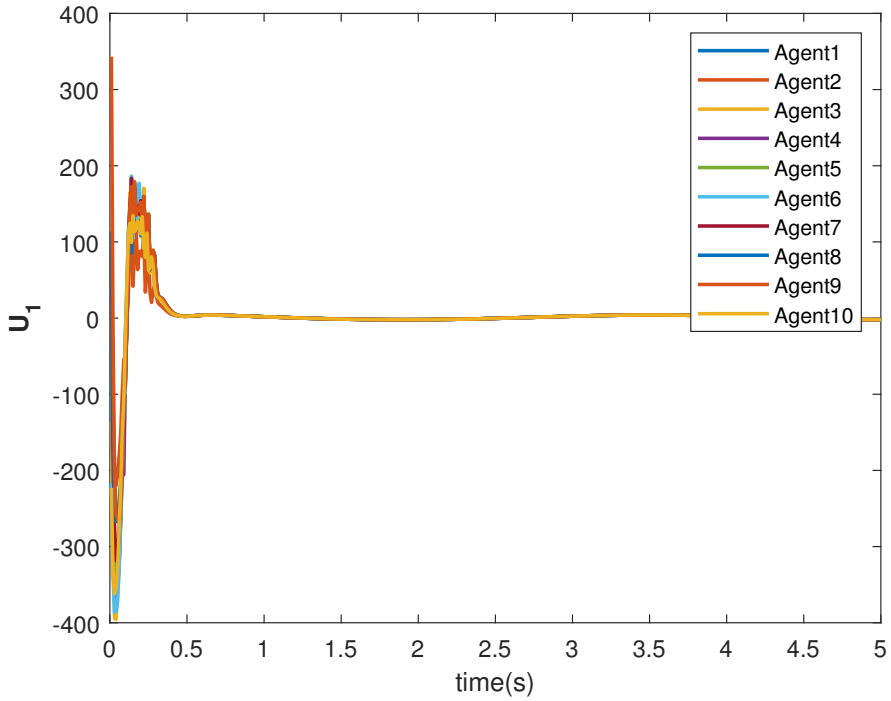

Figure 1. Control $\mathbf{U}_1$ of agents.

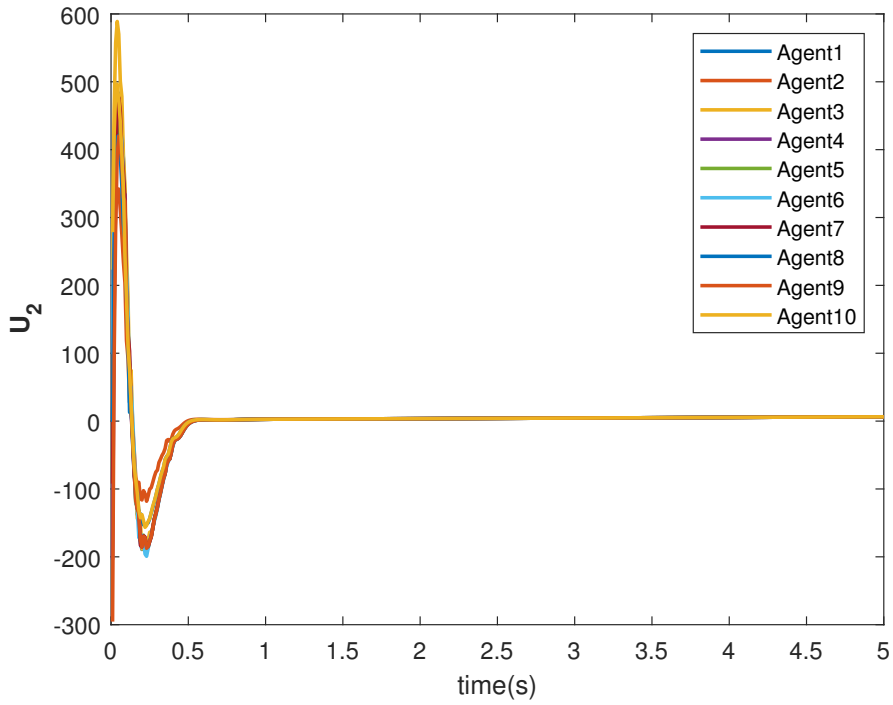

Figure 2. Control $\mathbf{U}_2$ of agents.

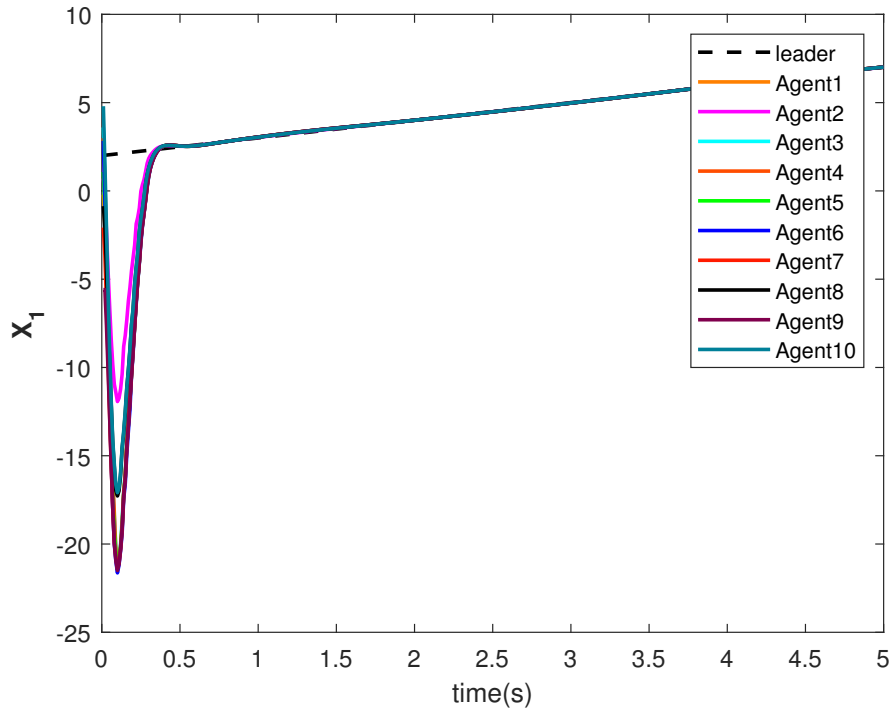

Figure 3. Consensus tracking of state $\mathbf{X}_1$ of the agents.

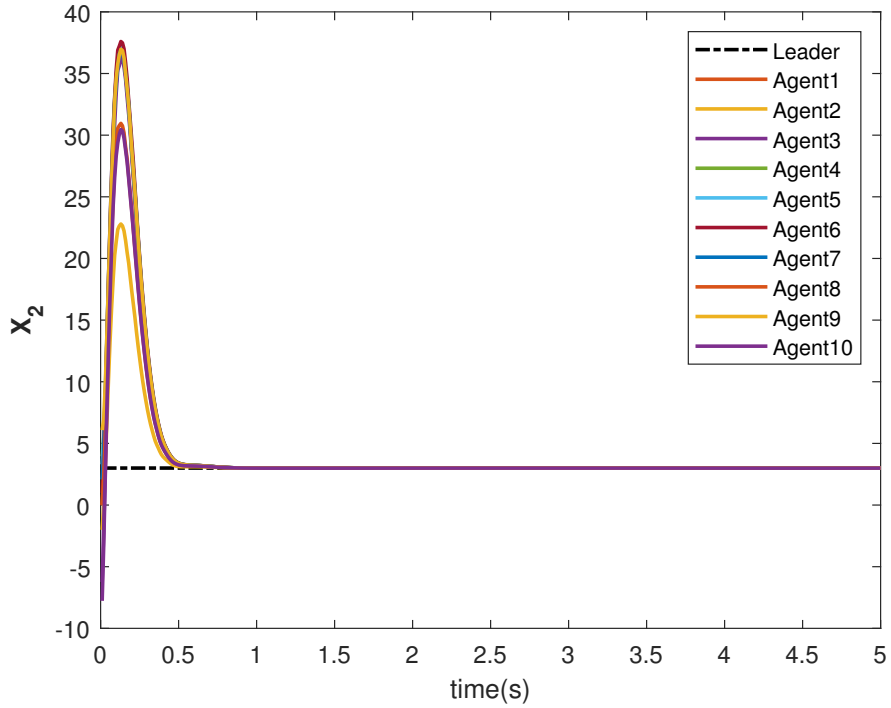

Figure 4. Consensus tracking of state $\mathbf{X}_2$ of the agents.

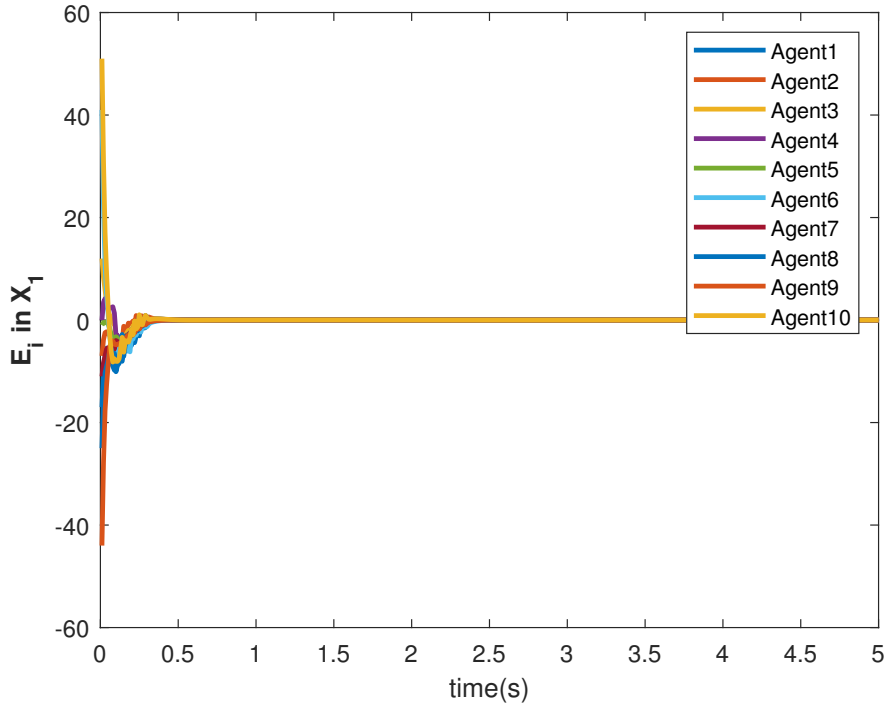

Figure 5. Consensus error $\mathbf{E}_i$ in state $\mathbf{X}_1$ of agents.

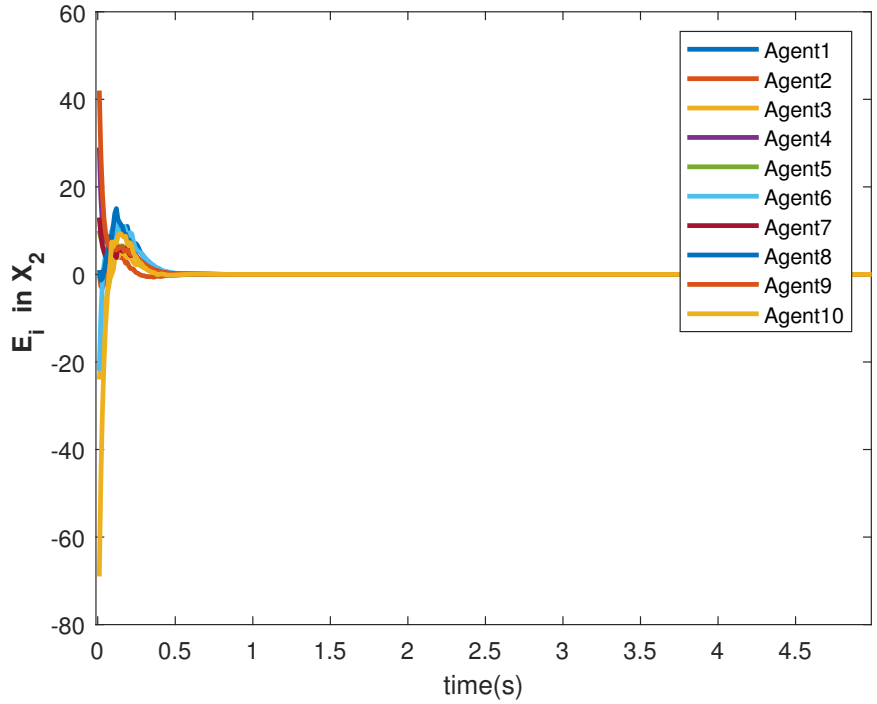

Figure 6. Consensus error $\mathbf{E}_2$ in state $\mathbf{X}_1$ of agents.

6.3.2. Case 2: Leader States-Sinusoid Function

In this case, the leader dynamics are considered as follows.

$$\dot{X}_{L_1} = 1.5X_{L_1}(t)\cos(2t+1) + X_{L_2}(t)\cos(4t) \quad (40)$$

$$\dot{X}_{L_2} = 2X_{L_2}(t)\sin(3t) \quad (41)$$

The consensus controls $\mathbf{U}_1$ and $\mathbf{U}_2$ are shown in Figures 7 and 8, respectively. It can be observed that the control signals are different from case 1. This is due to the leader's states, which are sinusoid in nature as given in Equations (40) and (41).

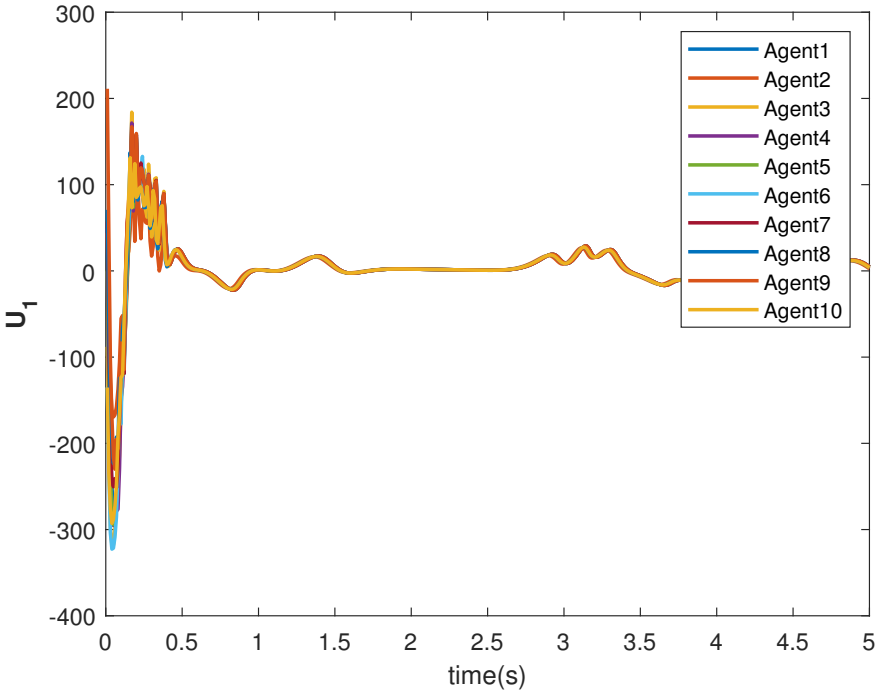

Figure 7. Control $\mathbf{U}_1$ of agents.

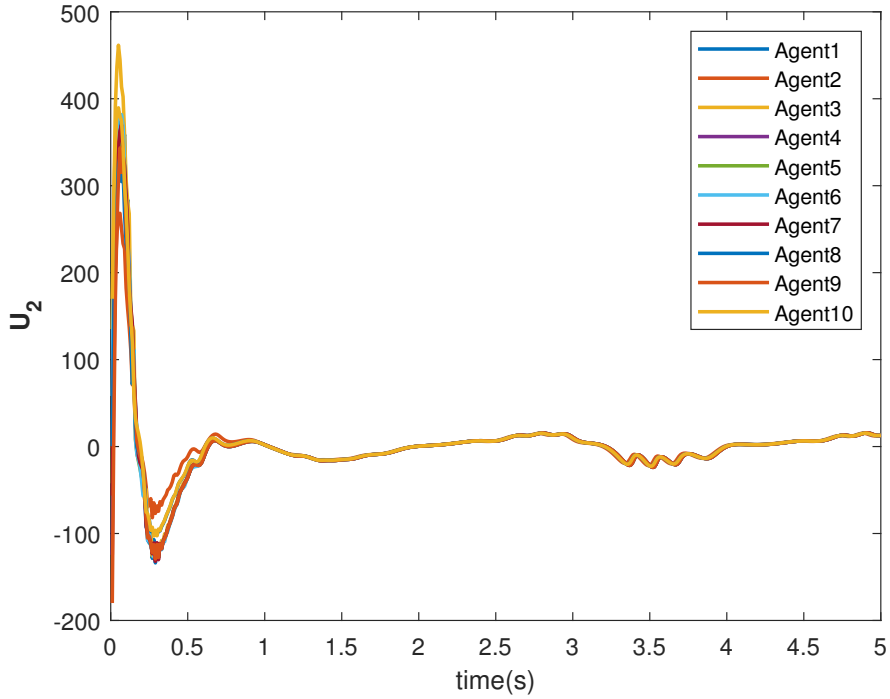

Figure 8. Control $\mathbf{U}_2$ of agents.

The state trajectories $\mathbf{X}_1$ and $\mathbf{X}_2$ are shown in Figures 9 and 10, respectively. The agents achieve consensus on the leader's trajectories. The leader's states are different, but the consensus controller has managed to track them.

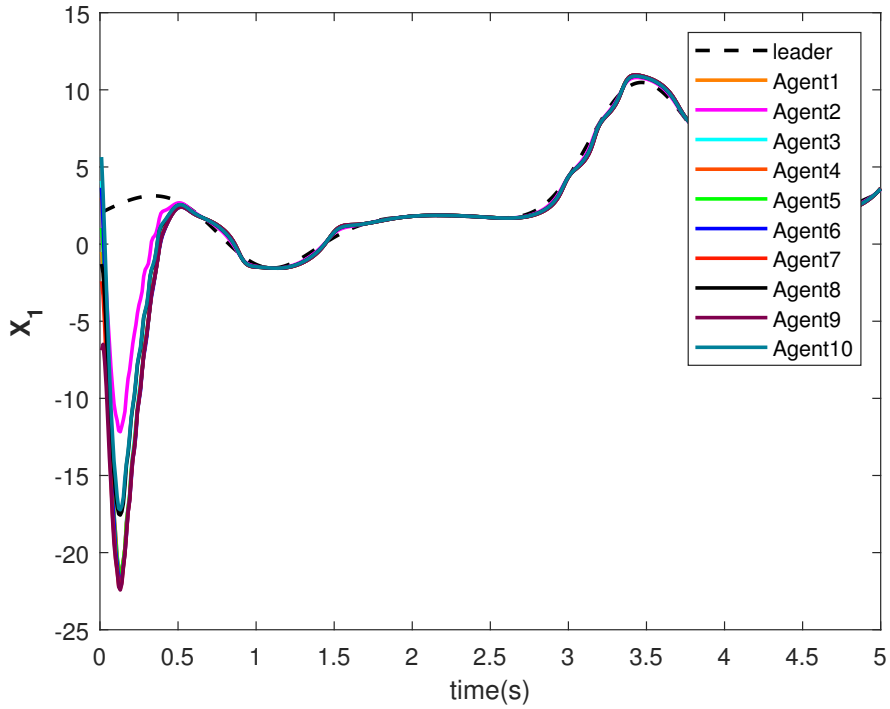

Figure 9. Consensus tracking of state $\mathbf{X}_1$ of the agents.

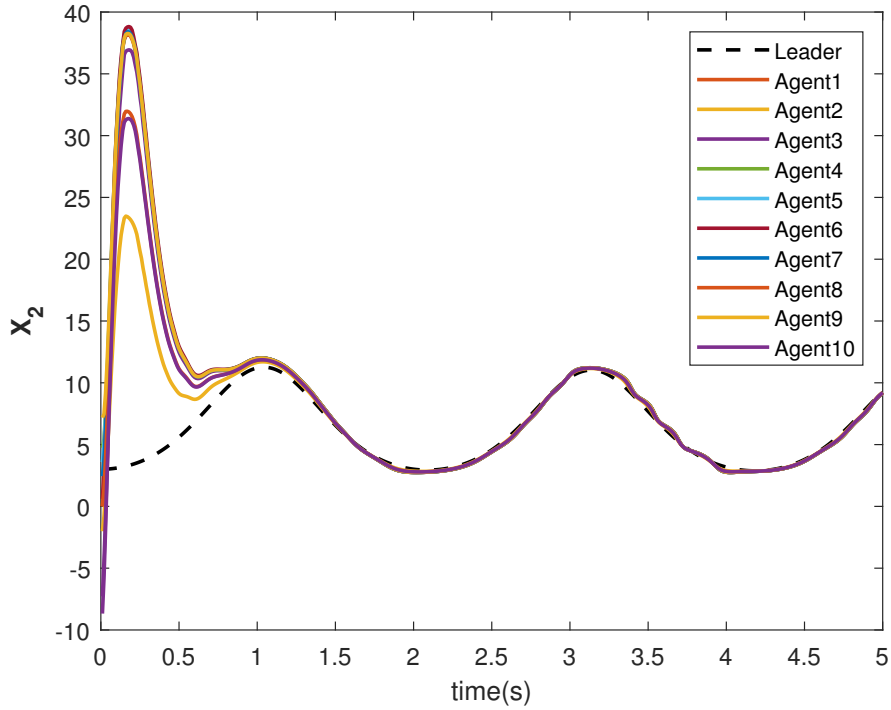

Figure 10. Consensus tracking of state $\mathbf{X}_2$ of the agents.

The accuracy of consensus tracking is described by the errors $\mathbf{E}_i$ in $\mathbf{X}_1$ and $\mathbf{X}_2$, which are shown in Figures 11 and 12, respectively. The consensus tracking errors become zero in a few seconds, which explains the effectiveness of the proposed controller.

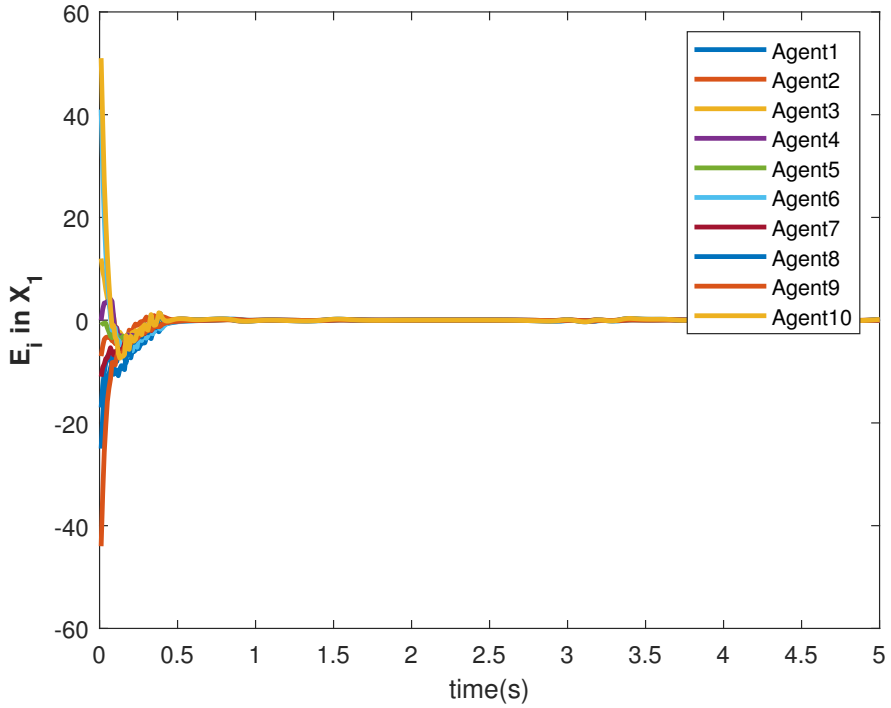

Figure 11. Consensus error $\mathbf{E}_i$ in state $\mathbf{X}_1$ of agents.

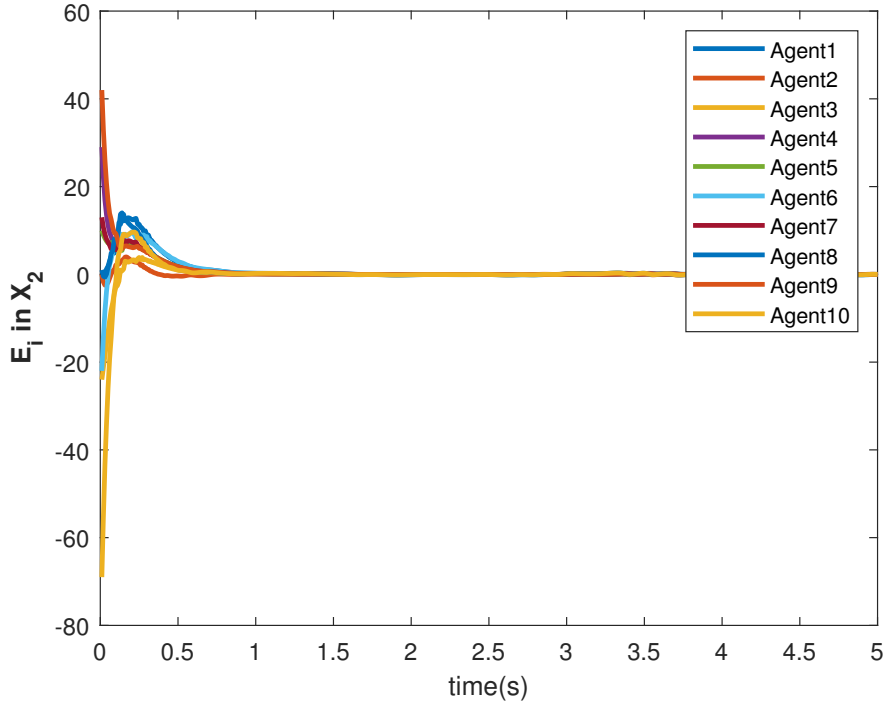

Figure 12. Consensus error $\mathbf{E}_2$ in state $\mathbf{X}_1$ of agents.

6.4. Results and Discussion: Switching Topology and Switching Leader-Follower Connections

In this case, we have presented the case where both (a) switching topology among the agents and (b) switching connection between the leader and the followers. The switching topologies are generated by the Algorithm 1.

Algorithm 1 Random topology generation.

for $k = 1$ to N_p **do**
  for $i = 1$ to N **do**
    for $j = 1$ to N **do**
      $x \leftarrow$ random number $x \in (0, 1)$
      if $x > 0.5$ **then**
        $A_k(i, j) \leftarrow 1$
        $A_k(j, i) \leftarrow 1$
      else
        $A_k(i, j) \leftarrow 0$
        $A_k(j, i) \leftarrow 0$
      end if
      if $i = j$ **then**
        $A_k(i, j) \leftarrow 0$
      end if
    end for
  end for
end for

We have generated N_p adjacency matrices, which denote the undirected topologies. N denotes the number of followers. The (i, j)th, $i, j = 1, 2, \ldots, N$ element of kth adjacency matrix $k = 1, 2, \ldots, N_p$ is generated depending on the value of a random variable x, which is mentioned in the Algorithm 1. One topology at each time instant is selected (denoted by A_s) randomly (among N_p topologies) using the Algorithm 2. A random integer *ind* in the range $[1, N_p]$ is selected, and the corresponding topology A_{ind} is chosen as A_s.

Algorithm 2 Selection of topology.

for $i = 1$ to T_s **do**
  $x \leftarrow$ random number $x \in (0, 1)$
  if $x > 0.5$ **then**
    $ind \leftarrow random\_integer([1\ N_p], 1)$
    $A_S \leftarrow A_{ind}$
  else
    A_S remains same
  end if
end for

T_s is the simulation time. Algorithms 1 and 2 were designed for implementing switching topology among the followers. Next, we will present the algorithms to describe the changing connections between the leader and the followers. N_L leader–follower connections are generated using Algorithm 3. It can be observed that each element of the array $temp$ is generated depending on the random variable x and a threshold value l. All the arrays generated are stored in the variable LF_con.

Algorithm 3 Switching leader–follower connection.

for $i = 1$ to N_L **do**
  for $j = 1$ to N **do**
    $x \leftarrow$ random number $x \in (0, 1)$
    if $x > l$ **then**
      $temp(j) \leftarrow 1$
    else
      $temp(j) \leftarrow 0$
    end if
  end for
  $LF\_con(i, :) \leftarrow temp$
end for

The leader–following switching connection is selected using the Algorithm 4. At each simulation time instant, one random integer ind is generated, and the array corresponding to ind in LF_con is selected as β. We considered the values of N_p and N_L as 100 and 30, respectively. The switching of topologies among the agents and switching connection of the leader–follower are shown in Figures 13 and 14, respectively. The topologies among the follower (given by the topology number) agents change at every time instant according to Algorithm 2. Similarly, the connections between the leader and the followers (given by the connection number) change according to Algorithm 4.

Algorithm 4 Selection of leader–follower connection.

for $i = 1$ to T_s **do**
  $x \leftarrow$ random number $x \in (0, 1)$
  if $x > l$ **then**
    $ind \leftarrow random\_integer([1\ N_L], 1)$
    $\beta \leftarrow LF\_con(ind, :)$
  else
    β remains same
  end if
end for

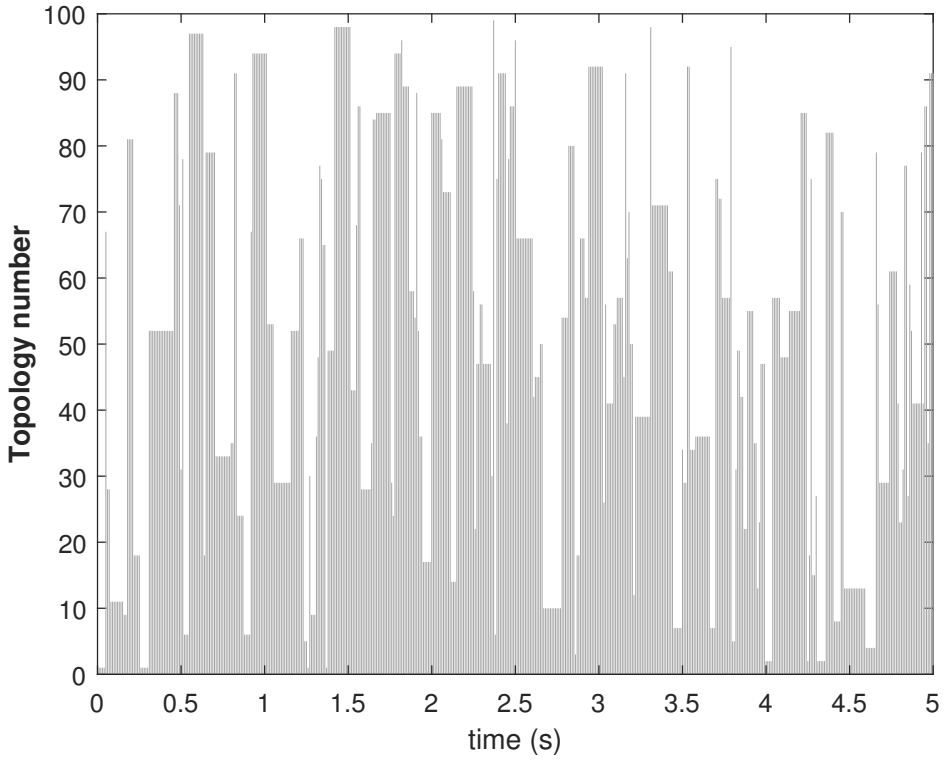

Figure 13. Consensus error $\mathbf{E}_i$ in state $\mathbf{X}_1$ of agents.

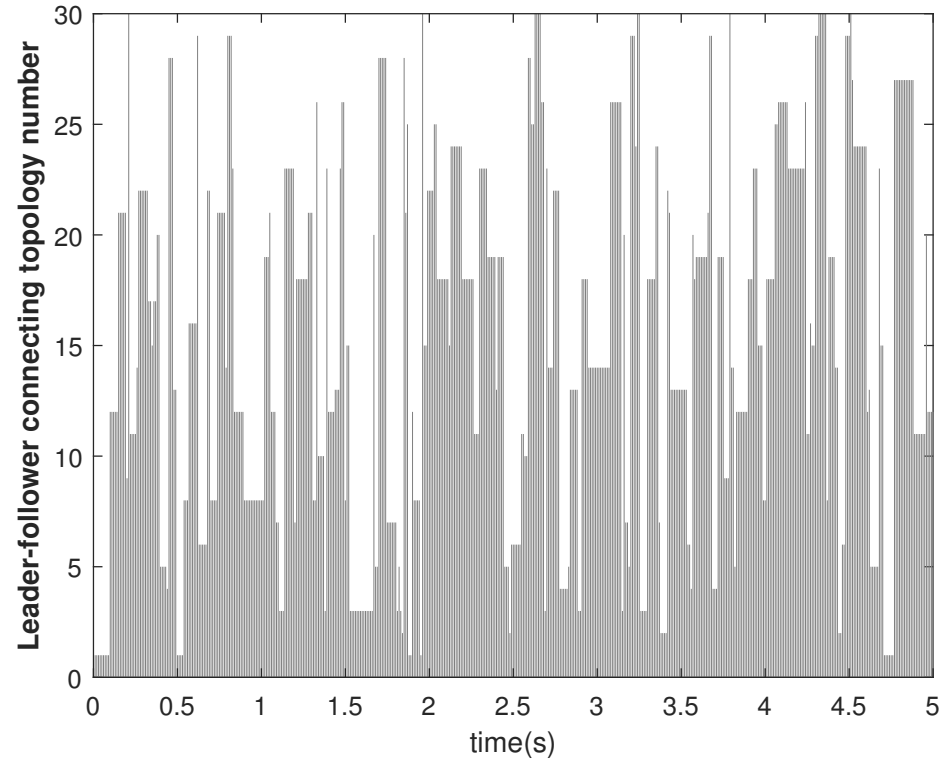

Figure 14. Consensus error $\mathbf{E}_2$ in state $\mathbf{X}_1$ of agents.

The tracking consensus controls $\mathbf{U}_1$ and $\mathbf{U}_2$ are shown in Figures 15 and 16, respectively. They have differences from other cases, which is the effect of the switching topology and connections.

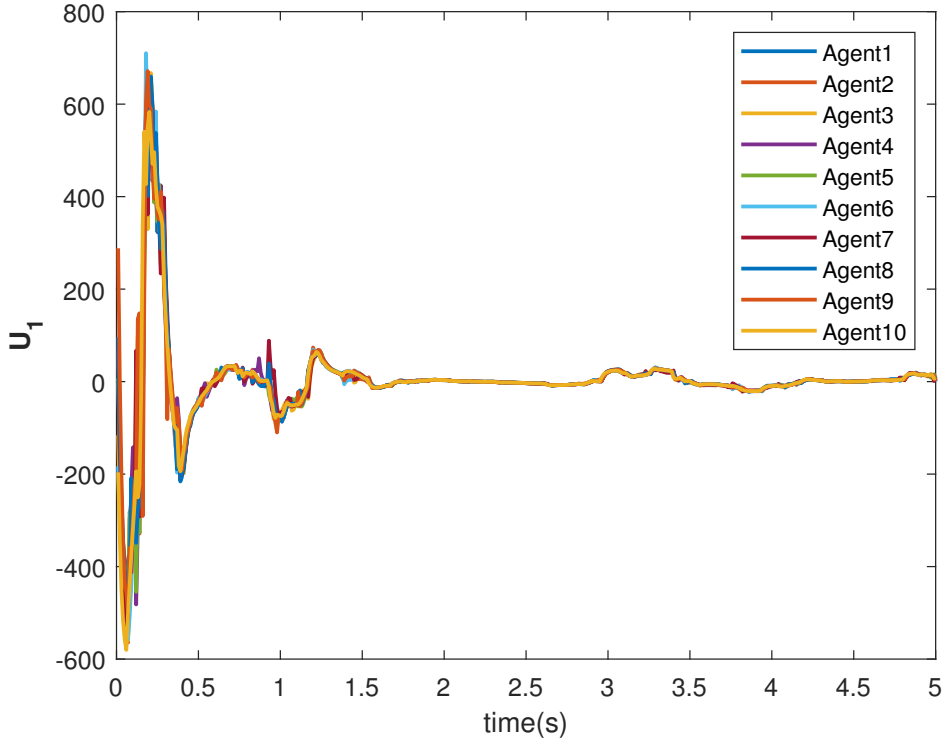

Figure 15. Control $\mathbf{U}_1$ of agents.

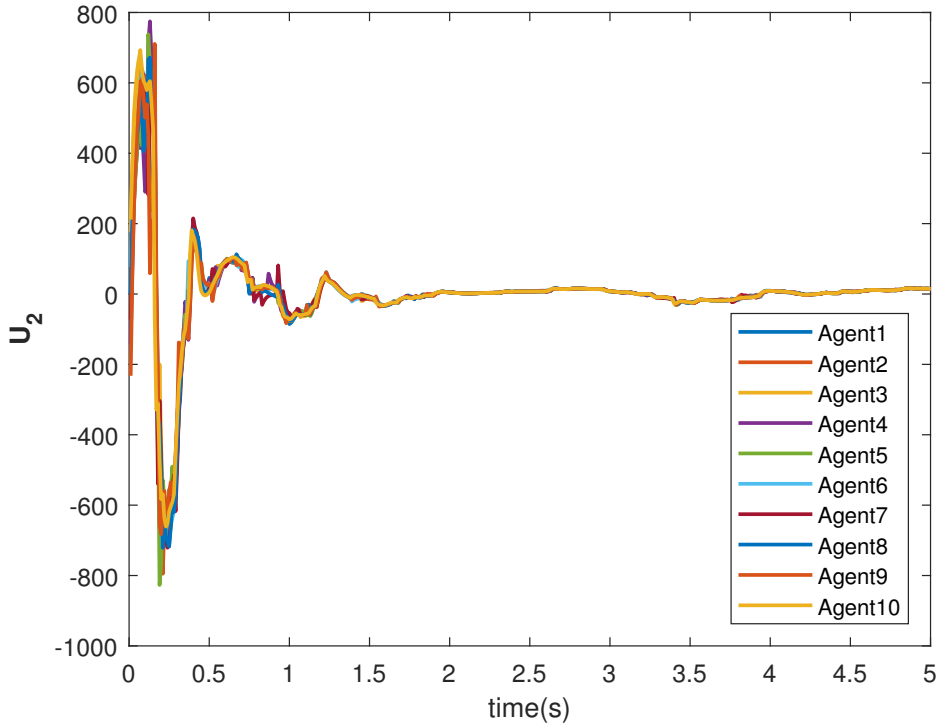

Figure 16. Control $\mathbf{U}_2$ of agents.

The state trajectories are generated by the control. The states of the followers started tracking efficiently within 2 s (see Figures 17 and 18). The effect of the switching is more visible within this time. However, the DNDI-based controller managed to reduce the error (see Figures 19 and 20) and improved the tracking performance. Therefore, it is clear that the proposed controller can perform the consensus tracking even in the presence of switching topology among followers and switching leader-follower connections.

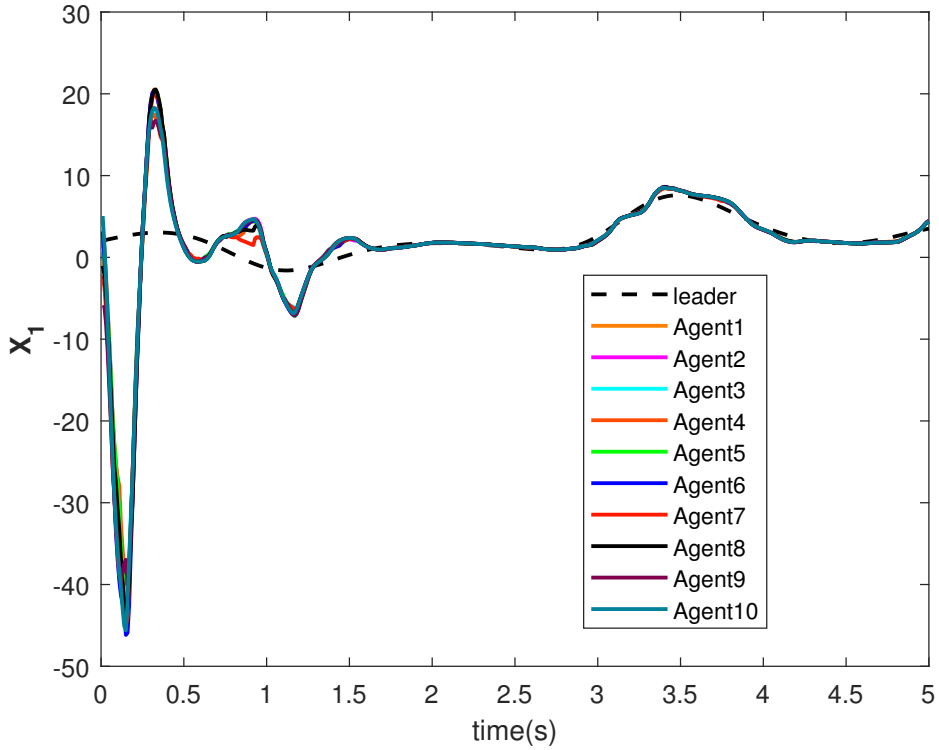

Figure 17. Consensus tracking of state $\mathbf{X}_1$ of the agents.

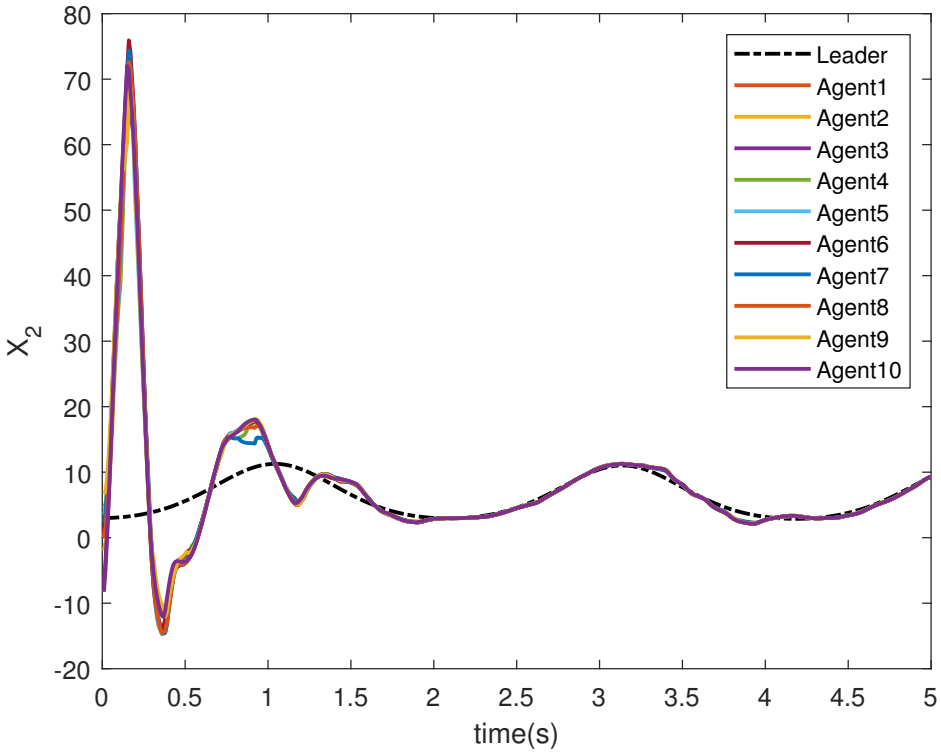

Figure 18. Consensus tracking of state $\mathbf{X}_2$ of the agents.

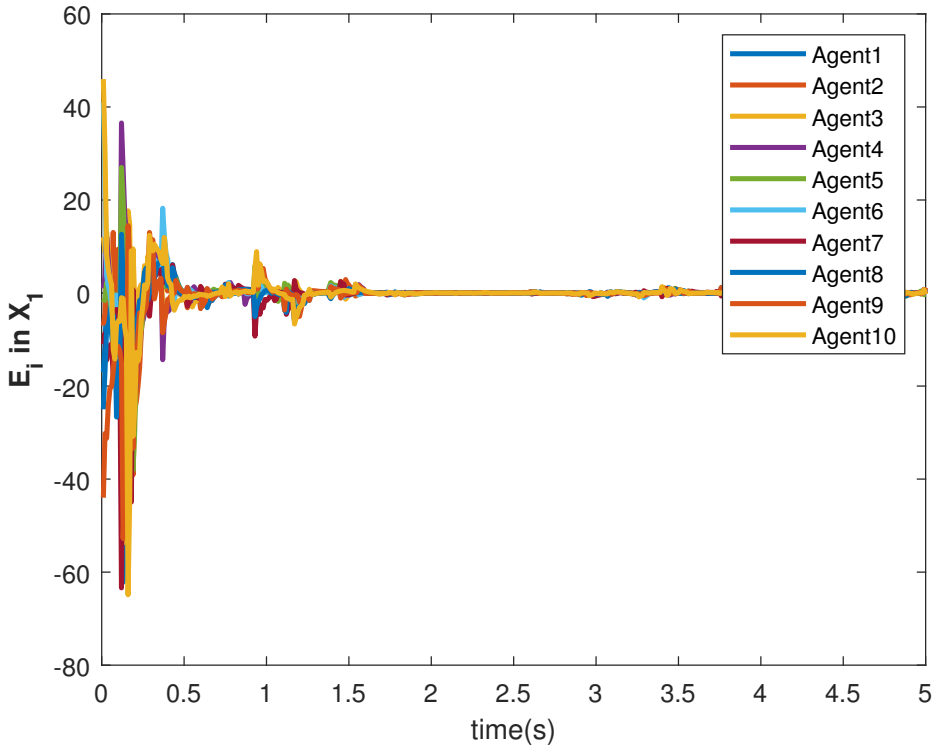

Figure 19. Consensus error $\mathbf{E}_i$ in state $\mathbf{X}_1$ of agents.

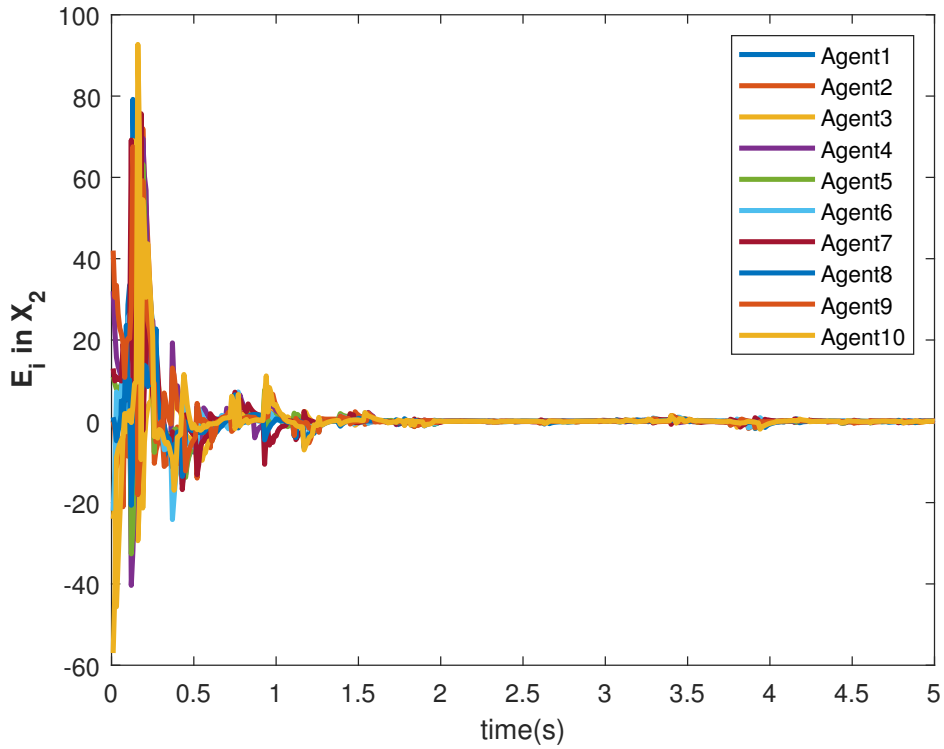

Figure 20. Consensus error $\mathbf{E}_2$ in state $\mathbf{X}_1$ of agents.

7. Conclusions

The DNDI-based fault-tolerant controller has been used to solve the consensus tracking control of nonlinear agents for the first time. This derivation is different compared to our previous work about leaderless consensus control. Moreover, switching topology among the agents and switching leader–follower connections are considered, which is

more realistic and addressed for the first time. A convergence study is presented to prove the tracking capability of the controller. A realistic simulation study evaluates the controller's performance, where different types of leader trajectories are generated, and the agents successfully track the leader's states. The results show that the proposed controller works efficiently in this realistic scenario. Therefore, the proposed controller is a potential candidate for consensus tracking applications.

Author Contributions: Conceptualization , S.M. and A.T.; methodology, S.M.; validation, S.M. and A.T.; writing–original draft preparation, S.M.; writing–review and editing, S.M. and A.T.; supervision, A.T.; project administration, A.T.; funding acquisition, A.T. All authors have read and agreed to the published version of the manuscript.

Funding: This research was partially funded by an Engineering and Physical Sciences Research Council (project: EP/R009953/1).

Data Availability Statement: No new data were created or analyzed in this study. Data sharing is not applicable to this article.

Conflicts of Interest: The authors declare no conflict of interest. The funders had no role in the design of the study; in the collection, analyses, or interpretation of data; in the writing of the manuscript, or in the decision to publish the results.

References

1. Cao, Y.U.; Kahng, A.B.; Fukunaga, A.S. Cooperative mobile robotics: Antecedents and directions. In *Robot Colonies*; Springer: Berlin/Heidelberg, Germany, 1997; pp. 7–27.
2. Florens, C.; Franceschetti, M.; McEliece, R.J. Lower bounds on data collection time in sensory networks. *IEEE J. Sel. Areas Commun.* **2004**, *22*, 1110–1120. [CrossRef]
3. Olfati-Saber, R. Flocking for multi-agent dynamic systems: Algorithms and theory. *IEEE Trans. Autom. Control* **2006**, *51*, 401–420. [CrossRef]
4. Ren, W.; Beard, R.W. *Distributed Consensus in Multi-Vehicle Cooperative Control*; Springer: Berlin/Heidelberg, Germany, 2008.
5. Gao, H.; Yang, X.; Shi, P. Multi-objective robust H_∞ Control of spacecraft rendezvous. *IEEE Trans. Control Syst. Technol.* **2009**, *17*, 794–802.
6. Wen, G.; Duan, Z.; Chen, G.; Yu, W. Consensus tracking of multi-agent systems with Lipschitz-type node dynamics and switching topologies. *IEEE Trans. Circuits Syst. I Regul. Pap.* **2013**, *61*, 499–511. [CrossRef]
7. Liu, W.; Zhou, S.; Qi, Y.; Wu, X. Leaderless consensus of multi-agent systems with Lipschitz nonlinear dynamics and switching topologies. *Neurocomputing* **2016**, *173*, 1322–1329. [CrossRef]
8. Zhao, H.; Peng, L.; Yu, H. Distributed model-free bipartite consensus tracking for unknown heterogeneous multi-agent systems with switching topology. *Sensors* **2020**, *20*, 4164. [CrossRef] [PubMed]
9. Xu, X.; Liu, L.; Feng, G. Consensus of single integrator multi-agent systems with unbounded transmission delays. *J. Syst. Sci. Complex.* **2019**, *32*, 778–788. [CrossRef]
10. Li, Y.; Yan, F.; Liu, W. Distributed consensus protocol for general third-order multi-agent systems with communication delay. In Proceedings of the 2019 Chinese Control And Decision Conference (CCDC), Nanchang, China, 3–5 June 2019; pp. 3436–3441.
11. Wang, A. Event-based consensus control for single-integrator networks with communication time delays. *Neurocomputing* **2016**, *173*, 1715–1719. [CrossRef]
12. Wang, Y.; Cheng, L.; Hou, Z.G.; Tan, M.; Zhou, C.; Wang, M. Consensus seeking in a network of discrete-time linear agents with communication noises. *Int. J. Syst. Sci.* **2015**, *46*, 1874–1888. [CrossRef]
13. Liu, J.; Ming, P.; Li, S. Consensus gain conditions of stochastic multi-agent system with communication noise. *Int. J. Control Autom. Syst.* **2016**, *14*, 1223–1230. [CrossRef]
14. Mondal, S.; Tsourdos, A. The consensus of non-linear agents under switching topology using dynamic inversion in the presence of communication noise and delay. *Proc. Inst. Mech. Eng. Part G J. Aerosp. Eng.* **2022**, *236*, 352–367. [CrossRef]
15. Liang, J.; Wang, Z.; Liu, Y.; Liu, X. Global synchronization control of general delayed discrete-time networks with stochastic coupling and disturbances. *IEEE Trans. Syst. Man Cybern. Part B (Cybernetics)* **2008**, *38*, 1073–1083. [CrossRef] [PubMed]
16. Mondal, S.; Tsourdos, A. Neuro-adaptive augmented distributed nonlinear dynamic inversion for consensus of nonlinear agents with unknown external disturbance. *Sci. Rep.* **2022**, *12*, 2049 . [CrossRef]
17. Tariverdi, A.; Talebi, H.A.; Shafiee, M. Fault-tolerant consensus of nonlinear multi-agent systems with directed link failures, communication noise and actuator faults. *Int. J. Control* **2019**, *94*, 60–74. [CrossRef]
18. Mondal, S.; Tsourdos, A. Fault-tolerant consensus of nonlinear agents considering switching topology in the presence of communication noise. *Proc. Inst. Mech. Eng. Part G J. Aerosp. Eng.* **2022**, *236*, 2776–2787. [CrossRef]
19. Jadbabaie, A.; Lin, J.; Morse, A.S. Coordination of groups of mobile autonomous agents using nearest neighbor rules. *IEEE Trans. Autom. Control* **2003**, *48*, 988–1001. [CrossRef]

20. Ren, W.; Beard, R.W. Consensus seeking in multiagent systems under dynamically changing interaction topologies. *IEEE Trans. Autom. Control* **2005**, *50*, 655–661. [CrossRef]
21. Ren, W. Multi-vehicle consensus with a time-varying reference state. *Syst. Control Lett.* **2007**, *56*, 474–483. [CrossRef]
22. Peng, K.; Yang, Y. Leader-following consensus problem with a varying-velocity leader and time-varying delays. *Phys. A Stat. Mech. Appl.* **2009**, *388*, 193–208. [CrossRef]
23. Cao, Y.; Ren, W. Distributed coordinated tracking with reduced interaction via a variable structure approach. *IEEE Trans. Autom. Control* **2011**, *57*, 33–48.
24. Hong, Y.; Wang, X.; Jiang, Z.P. Distributed output regulation of leader–follower multi-agent systems. *Int. J. Robust Nonlinear Control* **2013**, *23*, 48–66. [CrossRef]
25. Li, Z.; Ding, Z. Distributed adaptive consensus and output tracking of unknown linear systems on directed graphs. *Automatica* **2015**, *55*, 12–18. [CrossRef]
26. Wang, S.; Huang, J. Adaptive leader-following consensus for multiple Euler–Lagrange systems with an uncertain leader system. *IEEE Trans. Neural Netw. Learn. Syst.* **2018**, *30*, 2188–2196. [CrossRef] [PubMed]
27. Liu, J.; Zhang, Y.; Yu, Y.; Sun, C. Fixed-time leader–follower consensus of networked nonlinear systems via event/self-triggered control. *IEEE Trans. Neural Netw. Learn. Syst.* **2020**, *31*, 5029–5037. [CrossRef]
28. Lv, Y.; Wen, G.; Huang, T.; Duan, Z. Adaptive attack-free protocol for consensus tracking with pure relative output information. *Automatica* **2020**, *117*, 108998. [CrossRef]
29. Guo, W.; He, W.; Shi, L.; Sun, W.; Lu, X. Fixed-time consensus tracking for nonlinear stochastically disturbed multi-agent systems via discontinuous protocols. *Appl. Math. Comput.* **2021**, *400*, 126046. [CrossRef]
30. Yao, D.; Li, H.; Shi, Y. Adaptive Event-Triggered Sliding-Mode Control for Consensus Tracking of Nonlinear Multiagent Systems With Unknown Perturbations. *IEEE Trans. Cybern.* **2022**. [CrossRef]
31. Qin, J.; Zhang, G.; Zheng, W.X.; Kang, Y. Adaptive sliding mode consensus tracking for second-order nonlinear multiagent systems with actuator faults. *IEEE Trans. Cybern.* **2018**, *49*, 1605–1615. [CrossRef]
32. Mu, R.; Wei, A.; Li, H.; Yue, L. Leader-following consensus for multi-agent systems with actuator faults via adaptive event-triggered control. *J. Frankl. Inst.* **2021**, *358*, 1327–1349. [CrossRef]
33. Xiao, S.; Dong, J. Cooperative fault-tolerant fuzzy tracking control for nonlinear multiagent systems under directed network topology via a hierarchical control scheme. *Int. J. Robust Nonlinear Control* **2021**, *31*, 832–854. [CrossRef]
34. Gong, J.; Jiang, B.; Ma, Y.; Han, X.; Gong, J. Distributed adaptive fault-tolerant supervisory control for leader-following systems with actuator faults. *Int. J. Syst. Sci.* **2022**, *53*, 967–981. [CrossRef]
35. Wang, B.; Wang, J.; Zhang, B.; Chen, W.; Zhang, Z. Leader follower consensus of multivehicle wirelessly networked uncertain systems subject to nonlinear dynamics and actuator fault. *IEEE Trans. Autom. Sci. Eng.* **2017**, *15*, 492–505. [CrossRef]
36. Zou, W.; Ahn, C.K.; Xiang, Z. Fuzzy-approximation-based distributed fault-tolerant consensus for heterogeneous switched nonlinear multiagent systems. *IEEE Trans. Fuzzy Syst.* **2020**, *29*, 2916–2925. [CrossRef]
37. Wang, X.; Yang, G.H. Distributed H-infinity consensus tracking control for multi-agent networks with switching directed topologies. *Neurocomputing* **2016**, *207*, 693–699. [CrossRef]
38. Razaq, M.A.; Rehan, M.; Tufail, M.; Ahn, C.K. Multiple Lyapunov functions approach for consensus of one-sided Lipschitz multi-agents over switching topologies and input saturation. *IEEE Trans. Circuits Syst. II Express Briefs* **2020**, *67*, 3267–3271. [CrossRef]
39. Sader, M.; Liu, Z.; Wang, F.; Chen, Z. Distributed robust fault-tolerant consensus tracking control for multi-agent systems with exogenous disturbances under switching topologies. *Int. J. Robust Nonlinear Control* **2022**, *32*, 1618–1632. [CrossRef]
40. Liu, C.; Jiang, B.; Zhang, K.; Patton, R.J. Distributed fault-tolerant consensus tracking control of multi-agent systems under fixed and switching topologies. *IEEE Trans. Circuits Syst. I Regul. Pap.* **2021**, *68*, 1646–1658. [CrossRef]
41. Cao, Y.; Li, B.; Wen, S.; Huang, T. Consensus tracking of stochastic multi-agent system with actuator faults and switching topologies. *Inf. Sci.* **2022**, *607*, 921–930. [CrossRef]
42. Enns, D.; Bugajski, D.; Hendrick, R.; Stein, G. Dynamic inversion: An evolving methodology for flight control design. *Int. J. Control* **1994**, *59*, 71–91. [CrossRef]
43. Singh, S.; Padhi, R. Automatic path planning and control design for autonomous landing of UAVs using dynamic inversion. In Proceedings of the 2009 American Control Conference, St. Louis, MO, USA, 10–12 June 2009; pp. 2409–2414.
44. Lifeng, W.; Yichong, H.; Zhixiang, Z.; Congkui, H. Trajectory tracking of quadrotor aerial robot using improved dynamic inversion method. *Intell. Control. Autom.* **2013**, *2013*, 39495.
45. Mondai, S.; Padhi, R. Formation Flying using GENEX and Differential geometric guidance law. *IFAC-PapersOnLine* **2015**, *48*, 19–24. [CrossRef]
46. Caverly, R.J.; Girard, A.R.; Kolmanovsky, I.V.; Forbes, J.R. Nonlinear dynamic inversion of a flexible aircraft. *IFAC-PapersOnLine* **2016**, *49*, 338–342. [CrossRef]
47. Lombaerts, T.; Kaneshige, J.; Schuet, S.; Hardy, G.; Aponso, B.L.; Shish, K.H. Nonlinear Dynamic Inversion Based Attitude Control for a hovering quad tiltrotor eVTOL vehicle. In Proceedings of the AIAA Scitech 2019 Forum, San Diego, CA, USA, 7–11 January 2019; p. 0134.
48. Mondal, S.; Padhi, R. Constrained Quasi-Spectral MPSP With Application to High-Precision Missile Guidance With Path Constraints. *J. Dyn. Syst. Meas. Control* **2021**, *143*, 031001. [CrossRef]

49. Enenakpogbe, E.; Whidborne, J.F.; Lu, L. Control of an eVTOL using Nonlinear Dynamic Inversion. In Proceedings of the 2022 UKACC 13th International Conference on Control (CONTROL), Plymouth, UK, 20–22 April 2022; pp. 158–164.
50. Ma, X.; Liu, S.; Cheng, H. Civil aircraft fault tolerant attitude tracking based on extended state observers and nonlinear dynamic inversion. *J. Syst. Eng. Electron.* **2022**, *33*, 180–187. [CrossRef]
51. Saetti, U.; Rogers, J.D.; Alam, M.; Jump, M.; Cameron, N. Dynamic Inversion-Based Flare Control Law for Autonomous Helicopter Autorotation. In Proceedings of the AIAA SCITECH 2022 Forum, San Diego, CA, USA, 3–7 January 2022; p. 1645.
52. Mondal, S.; Tsourdos, A. Bipartite Consensus of Nonlinear Agents in the Presence of Communication Noise. *Sensors* **2022**, *22*, 2357. [CrossRef] [PubMed]
53. Ma, H.; Wang, Z.; Wang, D.; Liu, D.; Yan, P.; Wei, Q. Neural-network-based distributed adaptive robust control for a class of nonlinear multiagent systems with time delays and external noises. *IEEE Trans. Syst. Man Cybern. Syst.* **2015**, *46*, 750–758. [CrossRef]
54. Ge, S.S.; Wang, C. Adaptive neural control of uncertain MIMO nonlinear systems. *IEEE Trans. Neural Netw.* **2004**, *15*, 674–692. [CrossRef]

2022-12-06

Consensus tracking of nonlinear agents using distributed nonlinear dynamic inversion with switching leader-follower connection

Mondal, Sabyasachi

MDPI

Mondal S, Tsourdos A. (2022) Consensus tracking of nonlinear agents using distributed nonlinear dynamic inversion with switching leader-follower connection, Sensors, Volume 22, Issue 23, December 2022, Article number 9537

https://doi.org/10.3390/s22239537